

formers. This set consists of about  $2.78 \times 10^6$  conformers, the most abundant having a concentration of about 5%.<sup>25</sup> However, the rectangular conformer, which constitutes the low-temperature crystalline phase, is calculated to have a concentration of only about 1% in the liquid at 350 K. The set of diamond-lattice structures accounts for the fact that the spectrum of the liquid shows no evidence of individual conformers. In addition, the values of the probability ratios calculated on the basis of this set are in reasonably good agreement with the values obtained experimentally.

The distribution of conformers in the high-temperature crystalline mesomorphic phase was found to resemble that of the liquid for the three cycloalkanes we investigated. However, relative to the liquid, the distribution in the high-temperature solid appears to favor the lowest energy conformers. The lowest energy form [3434] of *c*-C<sub>14</sub>H<sub>28</sub> can be identified in the infrared spectra of both phases. For this cycloalkane, the high-temperature phase was estimated to contain about  $70 \pm 10\%$  [3434] in contrast to  $60 \pm 10\%$  for the liquid phase.

The vibrational spectra of *c*-C<sub>16</sub>H<sub>32</sub> and *c*-C<sub>22</sub>H<sub>44</sub> indicate that the conformer distribution in the high-temperature phase greatly resembles that of the liquid phase. However, there are significant differences between the two phases in the values of the ratios of the concentrations of short conformational sequences.

In the case of *c*-C<sub>22</sub>H<sub>44</sub>, the low-temperature, high-temperature, and liquid phases can be characterized in terms of their gauche bond content. The rings in the low-temperature phase each have

8 gauche bonds. The transition to the high-temperature phase results in an average increase of about 2 gauche bonds. The transition to the liquid adds about 1 more gauche bond. In these terms, the high-temperature phase is seen to be very much closer to the liquid than to the low-temperature phase.

**Acknowledgment.** We gratefully thank the National Institutes of Health, Grant GM 27690 to the University of California, Berkeley, and the National Science Foundation Polymers Program, Grant DMR 87-01586 to the University of California, Berkeley, and Grant DMR 86-96071 to the University of Akron, for supporting this research. We are indebted to Dr. Francis Jones of the Western Regional Research Center of the U.S. Department of Agriculture for help with the polarization microscopy on *c*-C<sub>22</sub>H<sub>44</sub>, to Dr. James Scherer of the same laboratory for help in measuring the Raman spectra of *c*-C<sub>16</sub>H<sub>32</sub>, and to Dr. Richard Twaddell of E. I. du Pont de Nemours, Wilmington, for measuring the enthalpies given in Table II. We also thank Dr. Yesook Kim for helping with some of the infrared and Raman measurements. Finally, we would like to express our deep thanks to Professor Martin Saunders of Yale University for furnishing us with the results of his calculations on the minimum energy structures of *c*-C<sub>14</sub>H<sub>28</sub> and *c*-C<sub>16</sub>H<sub>32</sub>.

**Registry No.** *c*-C<sub>16</sub>H<sub>32</sub>, 295-65-8; *c*-C<sub>22</sub>H<sub>44</sub>, 296-86-6; *c*-C<sub>14</sub>H<sub>28</sub>, 295-17-0; cyclohexadecane-1,1-*d*<sub>2</sub>, 118655-69-9; cyclodocosane-1,1-*d*<sub>2</sub>, 118681-72-4; cyclodocosanone, 59358-81-5; cyclohexadecanone, 2550-52-9.

## Spectroscopic Observation and Geometry Assignment of the Minimum Energy Conformations of Methoxy-Substituted Benzenes

P. J. Breen,<sup>1a,b</sup> E. R. Bernstein,<sup>\*,1a</sup> Henry V. Secor,<sup>1c</sup> and Jeffrey I. Seeman<sup>\*,1c</sup>

Contribution from the Department of Chemistry, Colorado State University, Fort Collins, Colorado 80523, and the Philip Morris Research Center, P.O. Box 26583, Richmond, Virginia 23261. Received April 14, 1988

**Abstract:** Optical spectroscopic data are presented for methoxybenzene, the three methoxytoluenes, 1-ethyl-4-methoxybenzene, and 1,2- and 1,3-dimethoxybenzene cooled and isolated in a supersonic jet expansion. Each unique stable conformation of the sterically unencumbered methoxybenzenes displays a unique and assignable spectrum; the interpretation of these spectra leads to the assignment of specific molecular geometries for each system. The minimum energy conformation of the methoxy group with respect to the ring is shown to be a planar conformation in which the methoxy group lies in the plane of the ring. The potential barrier for rotation of the ring methyl group in the methoxytoluenes is characterized from observed transitions between methyl group rotational levels which accompany the electronic transition. The meta isomer exhibits a large barrier to methyl rotation in S<sub>1</sub> ( $V_3 \sim 520 \text{ cm}^{-1}$ ) whereas the methyl group in the ortho and para isomers is nearly freely rotating ( $V_3 \leq 50 \text{ cm}^{-1}$ ). The dimethoxybenzenes exhibit spectral features due to torsions of the methoxy groups. Substantial barriers to methoxy group rotation ( $V_1 = 500 \text{ cm}^{-1}$ ,  $V_3 = 100 \text{ cm}^{-1}$  for ortho,  $V_1$  and  $V_3 \sim 2000\text{--}5000 \text{ cm}^{-1}$  for meta) are established; again the torsional barrier appears to be highest for the meta or 3-position on the ring. The presence of cross kinetic and potential terms between methoxy groups is further suggested for the ortho isomer.

### I. Introduction

The conformational preference of aromatic methyl ethers is a topic of significant current and fundamental interest.<sup>2-12</sup> While

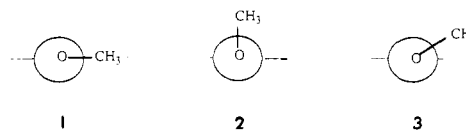
(1) (a) Colorado State University. (b) Current address: Baker Performance Chemicals, 3920 Essex Lane, Houston, TX 77027. (c) Philip Morris Research Center.

(2) Kruse, L. I.; DeBrosse, C. W.; Kruse, C. H. *J. Am. Chem. Soc.* **1985**, *107*, 5435.

(3) (a) Hummel, W.; Huml, K.; Bürgi, H.-B. *Helv. Chim. Acta* **1988**, *71*, 1291 and references cited therein; (b) Nyburg, S. C.; Faerman, C. H. *J. Mol. Struct.* **1986**, *140*, 347.

(4) Schaefer, T.; Salman, S. R.; Wildman, T. A.; Penner, G. H. *Can. J. Chem.* **1985**, *63*, 782.

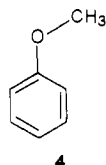
Chart I. Possible Conformations of Aromatic Methyl Ethers



the geometrical differences among various possible conformations of this substituent are large (see Chart I), the experimental de-

(5) Jardon, P. W.; Vickery, E. H.; Pahler, L. F.; Pourahmady, N.; Mains, G. J.; Eisenbraun, E. J. *J. Org. Chem.* **1984**, *49*, 2130.

termination of the ground-state energy minimum (or minima) for this or any aromatic substituent is extremely difficult.<sup>13-15</sup> Thus, even though recent NMR<sup>4-6</sup> and microwave<sup>7</sup> studies have agreed with theoretical treatments<sup>10-12</sup> that anisole (**4**) exists in the planar



**1** conformation, all the experimental evidence is *indirect*; that is, no reports of the observation of the individual "frozen-out" conformations of aromatic methyl ethers in either solution or gas phase have appeared.<sup>16</sup> In addition, the conformations of polysubstituted methoxybenzenes have been under some dispute in recent years.<sup>5,6,10,19,20</sup>

As illustrated in Chart I, three different conformations can be envisioned for aromatic methyl ethers: planar **1**, perpendicular **2**, and gauche **3**. One may contrast conformations **1-3** with the analogous conformations for aromatic compounds containing an aryl-to-primary alkyl group substituent (e.g., Ar-OCH<sub>3</sub> vs. Ar-CH<sub>2</sub>CH<sub>3</sub>). A perpendicular conformation is preferred in this latter set of compounds, presumably due to steric interactions between the C<sub>ortho</sub>-H and the alkyl side chain which apparently destabilize the planar conformation.<sup>15</sup>

As part of our studies on the conformations,<sup>21-26</sup> potential energy profiles,<sup>25,26</sup> and reactivities of aromatic compounds,<sup>26,27</sup> we have examined the absorption and emission spectra of a range of alkyl-substituted anisoles and 1,2- and 1,3-dimethoxybenzene. Two important features of this supersonic molecular jet laser spectroscopy, established in our previous studies,<sup>22-25</sup> must be emphasized. First, for the sterically unhindered molecules studied in this research, all conformers corresponding to stable potential energy minima, will be "frozen out" and trapped in the supersonic

(6) Rithner, C. D.; Bushweller, C. H.; Gensler, W. J.; Hoogasian, S. *J. Org. Chem.* **1983**, *48*, 1491.

(7) Onda, M.; Toda, A.; Mori, S.; Yamaguchi, I. *J. Mol. Struct.* **1986**, *144*, 47.

(8) Oikawa, A.; Abe, H.; Mikami, N.; Ito, M. *Chem. Phys. Lett.* **1985**, *116*, 50.

(9) Yamamoto, S.; Okuyama, K.; Mikami, N.; Ito, M. *Chem. Phys. Lett.* **1986**, *125*, 1.

(10) Makriyannis, A.; Fesik, S. *J. Am. Chem. Soc.* **1982**, *104*, 6462.

(11) Anderson, G. M., III; Kollman, P. A.; Domelsmith, L. N.; Houk, K. N. *J. Am. Chem. Soc.* **1979**, *101*, 2344.

(12) Korschin, H. *J. Mol. Struct. (THEOCHEM)* **1984**, *110*, 311.

(13) Ōki, M. *Applications of Dynamic NMR Spectroscopy to Organic Chemistry*; VCH Publishers: Deerfield Beach, FL, 1985.

(14) Jackman, L. M.; Cotton, F. M. *Dynamic NMR Spectroscopy*; Wiley: New York, 1975.

(15) Berg, U.; Liljefors, T.; Roussel, C.; Sandström, J. *Acc. Chem. Res.* **1985**, *18*, 80.

(16) Analyses of the crystal structures of molecules containing the methoxyphenyl substituent have been performed. For a large set of ortho-unsubstituted aryl methyl ethers, essentially planar conformation (cf. **1**) was observed.<sup>3</sup> The role of crystal packing and local repulsions in the crystal in forcing the methoxymethyl groups into the plane of the benzene ring has been discussed.<sup>17</sup> Some nonplanar conformations of *o*-dimethoxy aromatic compounds have been found in the crystal, although the majority of those studied were all planar.<sup>18</sup>

(17) Caillet, J. *Acta Crystallogr., Sect. B* **1982**, *38*, 1786.

(18) Faerman, C.; Nyburg, S. C.; Punte, G.; Rivero, B. E.; Vitale, A. A.; Nudelman, N. S. *Can. J. Chem.* **1985**, *63*, 3374.

(19) For additional results and leading references, see: Schaefer, T.; Laatikainen, R. *Can. J. Chem.* **1983**, *61*, 224.

(20) For a preliminary report of some of these results, see: Seeman, J. I.; Secor, H. V.; Breen, P. J.; Bernstein, E. R. *J. Chem. Soc., Chem. Commun.* **1988**, 393.

(21) Seeman, J. I. *Chem. Rev.* **1983**, *83*, 83.

(22) Breen, P. J.; Warren, J. A.; Bernstein, E. R.; Seeman, J. I. *J. Am. Chem. Soc.* **1987**, *109*, 3453.

(23) Breen, P. J.; Warren, J. A.; Bernstein, E. R.; Seeman, J. I. *J. Chem. Phys.* **1987**, *87*, 1927.

(24) Breen, P. J.; Bernstein, E. R.; Seeman, J. I. *J. Chem. Phys.* **1987**, *87*, 3269.

(25) Breen, P. J.; Warren, J. A.; Bernstein, E. R.; Seeman, J. I. *J. Chem. Phys.* **1987**, *87*, 1917.

(26) Seeman, J. I. *Pure Appl. Chem.* **1987**, *59*, 1661.

(27) For a review, see: Seeman, J. I. *Heterocycles* **1984**, *22*, 165.

TOFMS of methoxybenzene

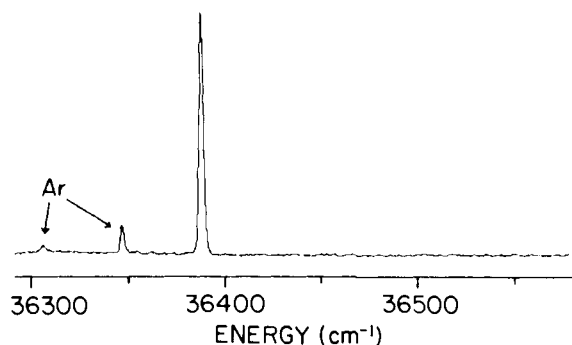


Figure 1. TOFMS of the 0<sub>0</sub><sup>0</sup> region of methoxybenzene. The single origin occurs at 36381.1 cm<sup>-1</sup> and indicates that only one stable conformation exists. The peaks indicated by "Ar" are due to absorptions by argon-methoxybenzene clusters which have dissociated and have been detected in the methoxybenzene mass channel.

DE of methoxybenzene

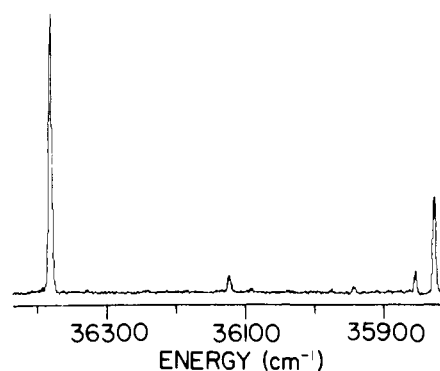


Figure 2. DE spectrum of the 0<sub>0</sub><sup>0</sup> region of methoxybenzene obtained by pumping the 36381.1-cm<sup>-1</sup> transition. The spectrum shows a lack of low-lying torsional modes of the methoxy group, as did Figure 1.

jet expansion. Second, the energy of the electronic 0<sub>0</sub><sup>0</sup> (origin) transition corresponds to a specific ground-state potential energy minimum conformation. The converse is also true; that is, each stable conformation generates its own origin transition.

In this work, we report the first observation of spectroscopic properties of specific energy minimum conformations for these aromatic methyl ethers.<sup>20</sup> Further, by observing the number of origins that occur in the spectra of these compounds, and by comparing this number with that predicted by the symmetries of each conformation (**1-3**), we are able to identify the geometry of the stable conformations.

In addition to the conformational analysis of the methoxy group, a methoxy torsional mode analysis is conducted for 1,2- and 1,3-dimethoxybenzene. Unlike the methyl anisoles and 1,4-dimethoxybenzene, these compounds exhibit spectroscopic features which are due to torsional transitions of the methoxy group. The potential parameters for this motion are evaluated using techniques and potential functions previously published.<sup>25</sup>

## II. Experimental Procedures

The time-of-flight mass spectrometer has been described previously.<sup>28</sup> The name "one (and two) color time-of-flight mass spectroscopy (TOFMS)" is generally employed to describe the following experiment. A sample is irradiated with a laser of energy  $\nu_1$  resulting in the generation of the first excited singlet state ( $S_0 \rightarrow S_1$ ). A second photon  $\nu_2$  subsequently ionizes those molecules in  $S_1$  ( $S_1 \rightarrow I^+$ ). The ions are detected in given mass channels by time-of-flight mass spectroscopy such that only ion current representing a chosen  $m/e$  is recorded. The energy of the  $\nu_1$  laser is changed, and an absorption spectrum of a mass-selected species is obtained. All photoionization spectra for these studies are two-photon,

(28) Bernstein, E. R.; Law, K.; Schauer, M. *J. Chem. Phys.* **1984**, *80*, 207.

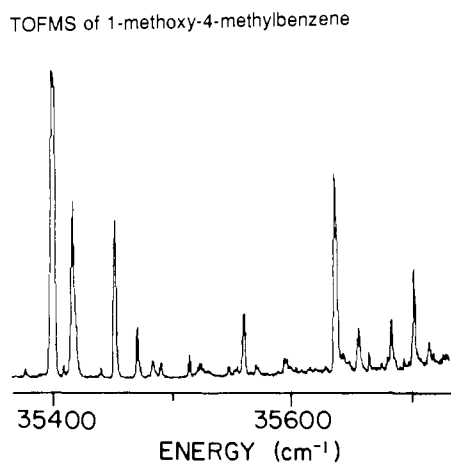


Figure 3. TOFMS of  $0_0^0$  region of 1-methoxy-4-methylbenzene. The peak at  $35400.4\text{ cm}^{-1}$  is assigned as the origin, while the features at  $35417.6$ ,  $35452.7$ , and  $35484.3\text{ cm}^{-1}$  are all assigned to internal rotational transitions of the ring methyl group. The intensity displayed by these latter features is unusual and indicates a change in geometry of the methyl group upon excitation from  $S_0$  to  $S_1$ .

one-color (i.e.,  $\nu_1 = \nu_2$ ). The dimethoxybenzenes are purchased from Wiley Organics Inc., and the methoxybenzene and methoxytoluenes are purchased from Aldrich. All are used without further purification. Experimental details for the preparation of 1-methoxy-3-(methyl- $d_3$ )-benzene<sup>29</sup> (**7**), 1-(methoxy- $d_3$ )-3-methylbenzene<sup>30</sup> (**8**), 1-methoxy-2-(methyl- $d_3$ )-benzene (**10**), 1-(methoxy- $d_3$ )-2-methylbenzene (**11**), and 1,2-di(methoxy- $d_3$ )-benzene<sup>31</sup> (**14**) are provided in the Supplementary Material.

Dispersed emission (DE) experiments are carried out in a fluorescence excitation (FE) chamber described previously.<sup>28</sup>  $f/4$  optics are used to collect and focus the emission onto the slits of an  $f/8$  2051 GCA McPherson 1-m scanning monochromator with a dispersion of  $2.78\text{ \AA}/\text{mm}$  in the third order of a 1200-groove/mm  $1\text{-}\mu\text{m}$  blazed grating.

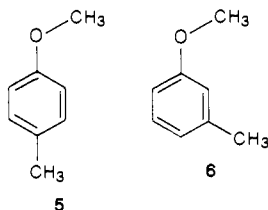
Expansion of the gas into the FE chamber is achieved with a Quanta Ray PSV-2 pulsed valve with a  $500\text{-}\mu$  pinhole located  $\sim 1\text{ cm}$  from the laser beam. The TOFMS experiments utilize a R. M. Jordan pulsed valve. Spectra are typically obtained using 30–50 psig of argon as the expansion carrier gas.

The potentials for internal rotation of the methoxy or methyl groups in the compounds studied are fit to observed spacings between features corresponding to internal rotational transitions using methods described in detail previously.<sup>25</sup>

### III. Results

**A. Anisole (4).** The TOFMS of the  $0_0^0$  region of the  $S_1 \leftarrow S_0$  for jet-cooled anisole (**4**), using 30 psig of argon as the carrier gas, is presented in Figure 1. The spectrum is featureless except for the single origin at  $36381.1\text{ cm}^{-1}$ . The DE spectrum obtained by pumping the  $0_0^0$  transition is presented in Figure 2, and is likewise devoid of features within  $200\text{ cm}^{-1}$  of the origin. The single origin presented in Figure 1 is evidence that only one minimum energy conformation of the methoxy group with respect to the ring exists.

**B. 1-Methoxy-4-methylbenzene (5).** Figure 3 displays the TOFMS of the  $0_0^0$  region of  $S_1 \leftarrow S_0$  for jet-cooled 1-methoxy-4-methylbenzene (**5**). The spectrum contains a single origin at



$35400.4\text{ cm}^{-1}$ , along with several intense features within  $100\text{ cm}^{-1}$

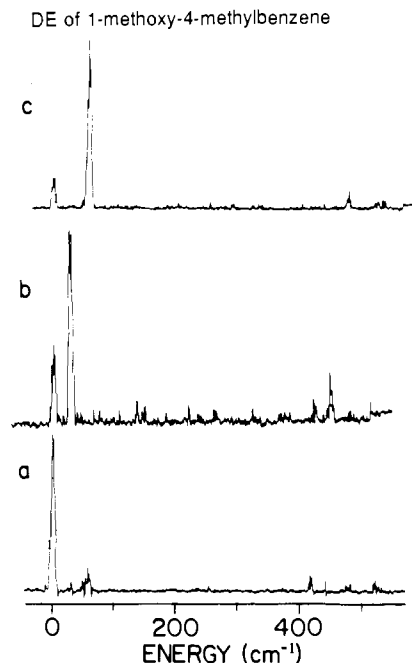


Figure 4. DE spectra of the  $0_0^0$  region of 1-methoxy-4-methylbenzene obtained by pumping the transitions in Figure 3 at (a)  $35400.4$ , (b)  $35417.6$ , and (c)  $35452.7\text{ cm}^{-1}$ . The spacings of the peaks in the spectra enable characterization of the ground-state potential for internal rotation of the ring methyl group.

Table I. Internal Rotational Levels for 1-Methoxy-4-methylbenzene in the  $S_0$  and  $S_1$  States

ground state $S_0^a$		excited state $S_1^b$	
level	energy ( $\text{cm}^{-1}$ )	level	energy ( $\text{cm}^{-1}$ )
0a <sub>1</sub>	0.00	0a <sub>1</sub>	0.00
1e	4.40	1e	5.47
2e	31.40	2e	21.96
3a <sub>2</sub>	60.25	3a <sub>2</sub>	46.75
3a <sub>1</sub>	60.26	3a <sub>1</sub>	52.33
4e	103.33	4e	88.12
5e	159.16	5e	137.53

<sup>a</sup>  $B = 6.23\text{ cm}^{-1}$ ,  $V_3 = 37.66\text{ cm}^{-1}$ ,  $V_6 = 6.35\text{ cm}^{-1}$ . <sup>b</sup>  $B = 5.49\text{ cm}^{-1}$ ,  $V_3 = 2.56\text{ cm}^{-1}$ ,  $V_6 = 11.20\text{ cm}^{-1}$ .

to higher energy of the origin. These latter features are assigned as transitions between internal rotational states of the ring methyl rotor in  $S_0$  and  $S_1$ .

In Figure 4, a–c are the DE spectra obtained by pumping the peaks (Figure 3) at  $35400.4$ ,  $35417.6$ , and  $35452.7\text{ cm}^{-1}$ , respectively. The spacings of the methyl rotor features in these spectra, together with those in Figure 3, can be fit by the energy levels listed in Table I and generated with the model parameters<sup>25</sup>  $B = 6.23\text{ cm}^{-1}$ ,  $V_3 = 37.66\text{ cm}^{-1}$ , and  $V_6 = 6.35\text{ cm}^{-1}$  for  $S_0$ , and  $B = 5.49\text{ cm}^{-1}$ ,  $V_3 = 2.56\text{ cm}^{-1}$ , and  $V_6 = 11.20\text{ cm}^{-1}$  for  $S_1$ . The calculated zero-point energies for  $S_0$  and  $S_1$  are  $18.84$  and  $6.78\text{ cm}^{-1}$ , respectively. The quality of the fit is illustrated in Table II, in which the allowed transitions along with their calculated and observed transition energies are listed for both excitation ( $S_1 \leftarrow S_0$ ) and DE ( $S_0 \leftarrow S_1$ ) experiments.

**C. 1-Methoxy-3-methylbenzene (6).** The TOFMS of the  $0_0^0$  region for  $S_1 \leftarrow S_0$  of jet-cooled 1-methoxy-3-methylbenzene (**6**) is presented in Figure 5. While the most intense and lowest energy feature at  $36047.5\text{ cm}^{-1}$  is readily identifiable as an origin, the assignment of the remaining portion of the spectrum is difficult without additional information. The series of intense features following the  $36047.5\text{ cm}^{-1}$  origin is most likely due to torsional motion of either the methoxy group or the ring methyl group approaching the harmonic (high barrier) limit, since the features appear to occur at fairly regular intervals.

Because molecular vibrations and internal rotations have fairly substantial isotope effects,<sup>32</sup> transitions between internal rotational

(29) Meyer, F.; Harrison, A. G. *Can. J. Chem.* **1964**, *42*, 2008.

(30) Korschin, H.; Tylli, H.; Westermark, B. *J. Mol. Struct.* **1983**, *102*, 279.

(31) Neugebauer, T. A.; Bamberger, S. *Chem. Ber.* **1974**, *107*, 2362.

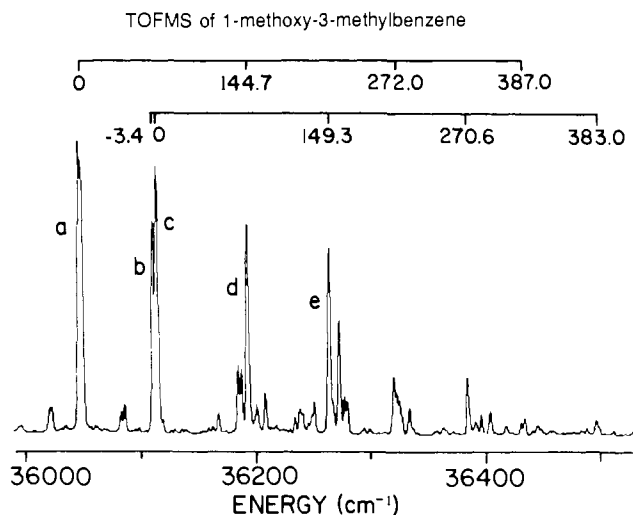
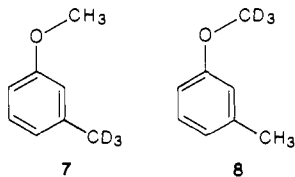


**Figure 5.** TOFMS of the  $0_0^0$  region of the 1-methoxy-3-methylbenzene. The features labeled a and b, at 36 047.5 and 36 113.8  $\text{cm}^{-1}$ , are assigned as origins belonging to separate conformations of the molecule. The ring methyl rotor in  $S_1$  experiences a large ( $\leq 525 \text{ cm}^{-1}$ ) barrier to rotation and is responsible for the indicated progressions of peaks built on the two origins in the spectrum.

**Table II.** Energies of Allowed Transitions between Internal Rotational Levels in the  $S_0$  and  $S_1$  States of 1-Methoxy-4-methylbenzene

transition ( $S_0 \leftarrow S_1$ )	calcd $E$ ( $\text{cm}^{-1}$ )	obsd $E$ ( $\text{cm}^{-1}$ ) by DE
$0a_1 \rightarrow 0a_1$	0.00	0
$0a_1 \rightarrow 3a_2$	60.25	60
$0a_1 \rightarrow 3a_1$	60.26	60
$1e \rightarrow 1e$	0.00	0
$1e \rightarrow 2e$	27.00	27
$1e \rightarrow 4e$	98.93	
transition ( $S_1 \leftarrow S_0$ )	calcd $E$ ( $\text{cm}^{-1}$ )	obsd $E$ ( $\text{cm}^{-1}$ ) by TOFMS
$0a_1 \rightarrow 0a_1$	0.00	0.0
$0a_1 \rightarrow 3a_2$	46.75	
$0a_1 \rightarrow 3a_1$	52.33	52.3
$1e \rightarrow 1e$	1.07	$0 \pm 1$
$1e \rightarrow 2e$	17.56	17.2
$1e \rightarrow 4e$	83.72	83.9

states of a methyl rotor can, in principle, show significant changes in spacings and intensities for the  $\text{CD}_3$  analogue. Thus, a comparison of the TOFMS of 3-methylanisole with that of its deuterated analogues (**7** and **8**) allows one to distinguish between



$S_1 \leftarrow S_0$  origin transitions for specific ground-state energy minima and transitions between internal rotational states of the methyl rotor(s). The TOFMS of 1-methoxy-3-(methyl- $d_3$ )benzene (**7**) is presented in Figure 6. Deuteriation of the methyl group produces a substantial change in the spacings and intensities of the peaks in Figure 6 relative to those in Figure 5, consistent with the notion that the majority of these features are due to transitions between internal rotational states of the methyl rotor.

One important similarity between Figures 5 and 6 is that they both contain a feature at  $\sim 64 \text{ cm}^{-1}$  to higher energy of the origins;

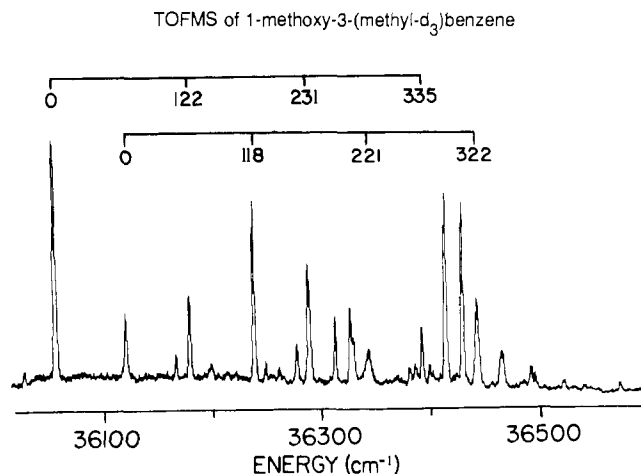


**Figure 6.** TOFMS of the  $0_0^0$  region of 1-methoxy-3-(methyl- $d_3$ )benzene. Deuteriation of the ring methyl group has reduced the spacings between peaks in the two progressions, indicating that these features are indeed due to torsional transitions of the ring methyl group. The two peaks assigned as origins, at 36 055.6 and 36 119.5  $\text{cm}^{-1}$ , remain  $64 \text{ cm}^{-1}$  apart in this spectrum. This spacing is also found for peaks a and b in Figure 5.

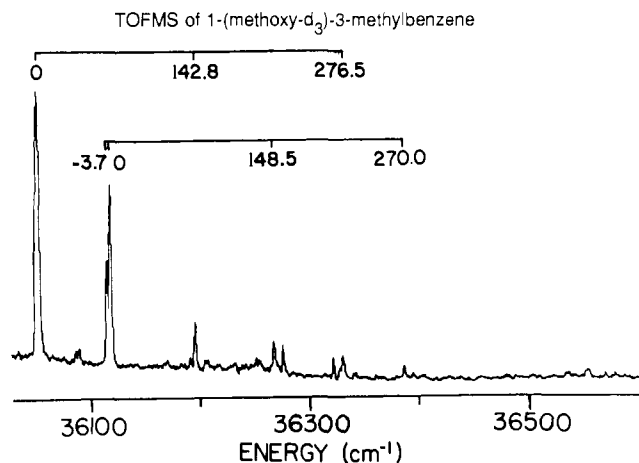


**Figure 7.** TOFMS of the  $0_0^0$  region of 1-(methoxy- $d_3$ )-3-methylbenzene. Deuteriation of the methoxy group has no effect on the spacings of the features in this spectrum relative to those in Figure 5, proving that transitions between internal rotational states of the methoxy group do not appear in the spectrum.

**Table III.** Internal Rotational Levels for 1-Methoxy-3-methylbenzene in the  $S_0$  and  $S_1$  State (Conformation I)

ground state $S_0^a$		excited state $S_1^b$	
level	energy ( $\text{cm}^{-1}$ )	level	energy ( $\text{cm}^{-1}$ )
$0a_1$	0.00	$0a_1$	0.00
$1e$	2.00	$1e$	0.00
$2e$	34.79	$2e$	143.40
$3a_2$	52.22	$3a_2$	143.55
$3a_1$	59.99	$3a_1$	270.85
$4e$	90.32	$4e$	272.32
$5e$	134.91	$5e$	376.11
$6a_2$	189.88	$6a_1$	389.07
$6a_1$	189.89	$6a_2$	444.56

<sup>a</sup>  $B = 5.03 \text{ cm}^{-1}$ ,  $V_3 = 58.78 \text{ cm}^{-1}$ ,  $V_6 = 1.04 \text{ cm}^{-1}$ . <sup>b</sup>  $B = 5.18 \text{ cm}^{-1}$ ,  $V_3 = 520.70 \text{ cm}^{-1}$ ,  $V_6 = 1.16 \text{ cm}^{-1}$ .

deuteriation has not caused this feature to shift in relative energy, although in Figure 6 it is no longer a doublet. This lack of a shift implies that the feature at  $64 \text{ cm}^{-1}$  is either a separate origin or a torsional feature of the methoxy group. Figure 7 displays the spectrum of 1-(methoxy- $d_3$ )-3-methylbenzene (**8**) in this region. Since this spectrum is virtually identical with that of Figure 5 in terms of spacings between peaks, the  $64\text{-cm}^{-1}$  feature must be a separate origin, and the remaining features must be due to torsional

**Table IV.** Energies of Allowed Transitions between Internal Rotational Levels in the  $S_0$  and  $S_1$  States of 1-Methoxy-3-methylbenzene (Conformation I)

transition ( $S_0 \leftarrow S_1$ )	calcd $E$ ( $\text{cm}^{-1}$ )	obsd $E$ ( $\text{cm}^{-1}$ ) by DE
$0a_1 \rightarrow 0a_1$	0.00	0
$0a_1 \rightarrow 3a_2$	52.22	
$0a_1 \rightarrow 3a_1$	59.99	60
$1e \rightarrow 1e$	0.00	0
$1e \rightarrow 2e$	32.79	
$1e \rightarrow 4e$	88.32	

transition ( $S_1 \leftarrow S_0$ )	calcd $E$ ( $\text{cm}^{-1}$ )	obsd $E$ ( $\text{cm}^{-1}$ ) by TOFMS
$0a_1 \rightarrow 0a_1$	0.00	0.0
$0a_1 \rightarrow 3a_2$	143.55	144.7
$0a_1 \rightarrow 3a_1$	270.85	272.0
$1e \rightarrow 1e$	-2.00	
$1e \rightarrow 2e$	141.40	144.7
$1e \rightarrow 4e$	270.32	272.0
$1e \rightarrow 5e$	374.11	387.0

**Table V.** Internal Rotational Levels for 1-Methoxy-3-methylbenzene in the  $S_0$  and  $S_1$  States (Conformation II)

ground state $S_0^a$		excited state $S_1^b$	
level	energy ( $\text{cm}^{-1}$ )	level	energy ( $\text{cm}^{-1}$ )
$0a_1$	0.00	$0a_1$	0.00
$1e$	3.40	$1e$	0.00
$2e$	28.50	$2e$	149.56
$3a_2$	51.37	$3a_2$	149.64
$3a_1$	54.00	$3a_1$	280.81
$4e$	89.35	$4e$	282.35
$5e$	136.96	$5e$	387.58
		$6a_2$	401.35
		$6a_1$	455.83

<sup>a</sup> $B = 5.32 \text{ cm}^{-1}$ ,  $V_3 = 38.22 \text{ cm}^{-1}$ ,  $V_6 = 2.02 \text{ cm}^{-1}$ . <sup>b</sup> $B = 5.29 \text{ cm}^{-1}$ ,  $V_3 = 532.84 \text{ cm}^{-1}$ ,  $V_6 = 9.33 \text{ cm}^{-1}$ .

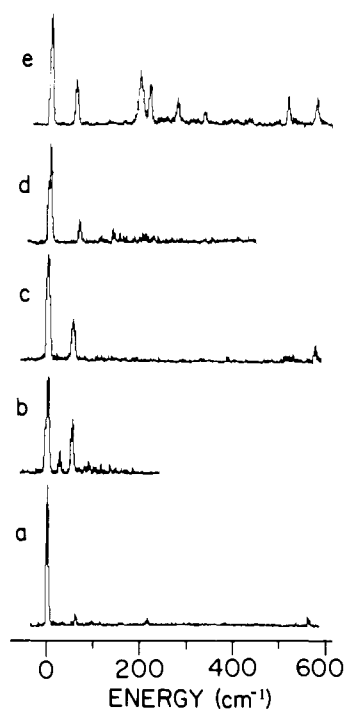
transitions of the ring methyl group.

The first identifiable methyl rotor transition in Figure 5 is the feature occurring  $144.7 \text{ cm}^{-1}$  to higher energy of the  $36047.5 \text{ cm}^{-1}$  origin. This peak shifts upon deuteration of the ring methyl group. This feature, together with those at  $272$  and  $387 \text{ cm}^{-1}$  from the origin, appear to form a progression which can be fit with the energy levels listed in Table III for  $S_1$  conformation I. The fitted potential parameters are  $B = 5.18 \text{ cm}^{-1}$  and  $V_3 = 520.70 \text{ cm}^{-1}$ , with a resulting zero-point energy of  $75.16 \text{ cm}^{-1}$ . The calculated and observed transition energies for these parameters are listed in Table IV and match the observed spacings well.

A similar progression of features is built on the  $64 \text{ cm}^{-1}$  origin (at  $36113.8 \text{ cm}^{-1}$  in Figure 5), with peaks spaced at intervals of  $149.3$ ,  $270.6$ , and  $383 \text{ cm}^{-1}$  to higher energy. This origin and subsequent methyl rotor progression are associated with another conformer of 1-methoxy-3-methylbenzene, designated as conformation II. The progression can be fit with the energy levels listed in Table V for  $S_1$  with the potential parameters  $B = 5.29 \text{ cm}^{-1}$ ,  $V_3 = 532.84 \text{ cm}^{-1}$ , and  $V_6 = 9.33 \text{ cm}^{-1}$ . The calculated zero-point energy is  $78.76 \text{ cm}^{-1}$ . The calculated and observed transition energies for conformation II are listed in Table VI.

The DE spectra associated with pumping the features labeled a-e in Figure 5 are presented in Figure 8a-e, respectively. In Figure 8, a and d are the DE spectra associated with the first origin (conformation I) at  $36047.5 \text{ cm}^{-1}$  in Figure 5. The fact that this origin is not a resolved doublet places an upper limit of ca.  $2 \text{ cm}^{-1}$  on the difference in energy between the  $0a_1 \rightarrow 0a_1$  and  $1e \rightarrow 1e$  levels in  $S_0$  is within ca.  $2 \text{ cm}^{-1}$  of what it is in  $S_1$  ( $\sim 0 \text{ cm}^{-1}$ ). The feature at  $60 \text{ cm}^{-1}$  is assigned to the  $0a_1 \rightarrow 3a_1$  transition. A reasonable set of model parameters which fits these two requirements for the energy levels in  $S_0$  is presented in Table III. The parameters are  $B = 5.03 \text{ cm}^{-1}$ ,  $V_3 = 58.78 \text{ cm}^{-1}$ , and  $V_6 = 1.04 \text{ cm}^{-1}$ , with a calculated zero-point energy of  $21.60 \text{ cm}^{-1}$ .

DE of 1-methoxy-3-methylbenzene

**Figure 8.** DE spectra of the  $0_0^0$  region for  $S_0 \leftarrow S_1$  of 1-methoxy-3-methylbenzene, obtained by pumping the transitions labeled a-e in Figure 5. Features within the first  $100 \text{ cm}^{-1}$  of the origins are assigned as ring methyl rotor transitions, and are used to characterize the potential well for methyl rotation in  $S_0$ .**Table VI.** Energies of Allowed Transitions between Internal Rotational Levels in the  $S_0$  and  $S_1$  States of 1-Methoxy-3-methylbenzene (Conformation II)

transition ( $S_0 \leftarrow S_1$ )	calcd $E$ ( $\text{cm}^{-1}$ )	obsd $E$ ( $\text{cm}^{-1}$ ) by DE
$0a_1 \rightarrow 0a_1$	0.00	0
$0a_1 \rightarrow 3a_2$	51.37	
$0a_1 \rightarrow 3a_1$	54.00	54
$1e \rightarrow 1e$	0.00	0
$1e \rightarrow 2e$	25.10	27
$1e \rightarrow 4e$	85.95	

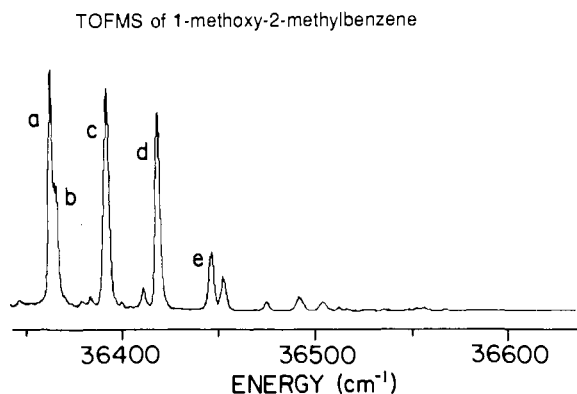
  

transition ( $S_1 \leftarrow S_0$ )	calcd $E$ ( $\text{cm}^{-1}$ )	obsd $E$ ( $\text{cm}^{-1}$ ) by TOFMS
$0a_1 \rightarrow 0a_1$	0.00	0.0
$0a_1 \rightarrow 3a_2$	149.64	149.3
$0a_1 \rightarrow 3a_1$	280.81	270.6
$1e \rightarrow 1e$	-3.40	-3.4
$1e \rightarrow 2e$	146.16	149.3
$1e \rightarrow 4e$	278.95	270.6
$1e \rightarrow 5e$	384.18	383.0

Table IV lists the calculated and observed transition energies and illustrates the goodness of the fit for  $S_0$  and  $S_1$ .

In Figure 8, b, c, and e are all associated with the origin at  $36113.8 \text{ cm}^{-1}$  (conformation II). The features at  $27$  and  $\sim 54 \text{ cm}^{-1}$  from the origins in Figure 8 (b, c, and e) are assigned as methyl rotor transitions and can be fit by the energy levels listed in Table V for  $S_0$  for conformation II. The fitted potential parameters are  $B = 5.32 \text{ cm}^{-1}$ ,  $V_3 = 38.22 \text{ cm}^{-1}$ , and  $V_6 = 0 \text{ cm}^{-1}$ . The calculated zero-point energy is  $16.48 \text{ cm}^{-1}$ . The calculated and observed transition energies are listed in Table VI.

From Table V (conformation II), the difference in energy between the  $0a_1 \rightarrow 0a_1$  and  $1e \rightarrow 1e$  methyl rotor transitions is  $\sim 3.4 \text{ cm}^{-1}$ . This spacing is responsible for the observed doublet at the origin. The red component of this doublet, at  $36110.4 \text{ cm}^{-1}$ , is due to the  $1e \rightarrow 1e$  transition, and the other, higher energy



**Figure 9.** TOFMS of the  $0_0^0$  region of 1-methoxy-2-methylbenzene peak "a" is assigned to be an origin and occurs at  $36\ 101.5\ \text{cm}^{-1}$ . The peaks labeled b–e are all assigned to be ring methyl rotor rotational transitions.

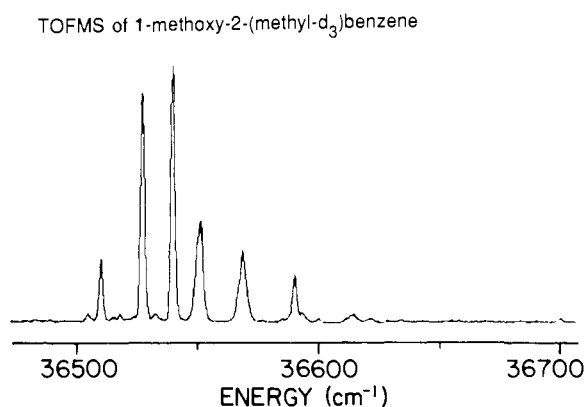
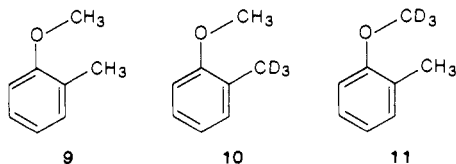


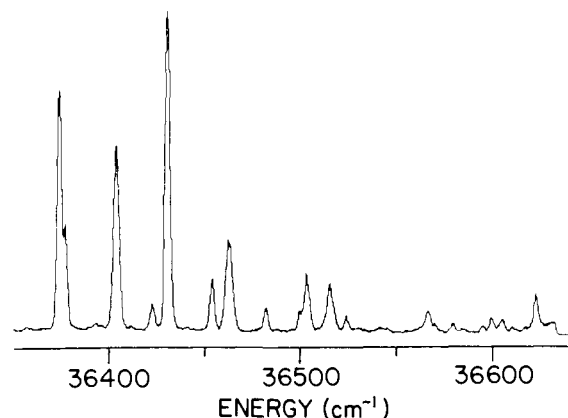
**Figure 10.** TOFMS of the  $0_0^0$  region of 1-methoxy-2-(methyl- $d_3$ )benzene. The origin occurs at  $35\ 403.5\ \text{cm}^{-1}$ . The features to the blue of the origin have all shifted closer together upon deuteration than those associated with the protonated compound (Figure 9). Such shifts support the assignment of these features to ring methyl rotational transitions.

component at  $36\ 113.8\ \text{cm}^{-1}$  is the true origin corresponding to the  $0a_1 \rightarrow 0a_1$  transition. Upon deuteration of the ring methyl group, the rotational constant  $B$  is reduced by a factor of 2, and the spacing between the  $1e \rightarrow 1e$  and  $0a_1 \rightarrow 0a_1$  transitions is reduced to  $0.77\ \text{cm}^{-1}$  (calculated) so that the origin (conformation II) in Figure 6 no longer appears as a resolved doublet.

**D. 1-Methoxy-2-methylbenzene (9).** The TOFMS of the  $0_0^0$  region for  $S_1 \leftarrow S_0$  for jet-cooled 1-methoxy-2-methylbenzene (**9**) is presented in Figure 9. The first and most intense feature of the spectrum occurs at  $36\ 364.6\ \text{cm}^{-1}$  and is assigned to be an origin. The remaining intense features of the spectrum spaced at  $28.9$ ,  $55.3$ , and  $81.1\ \text{cm}^{-1}$  to higher energy of the origin could be other origins corresponding to different conformers of the molecule or could be due to transitions between internal rotational states of the ring methyl or methoxy groups. To distinguish between these alternatives, we have prepared two deuteriated analogues of 1-methoxy-2-methylbenzene, namely, **10** and **11**.



The TOFMS of the  $0_0^0$  region for  $S_1 \leftarrow S_0$  for jet-cooled 1-methoxy-2-(methyl- $d_3$ )benzene (**10**) is presented in Figure 10. Deuteration of the methyl group of **9** causes the features at  $28.9$ ,  $55.3$ , and  $81.1\ \text{cm}^{-1}$  from the origin in Figure 9 to shift closer to the origin, as shown in Figure 10. Such a shift implies that these features are indeed transitions between various torsional levels of the ring methyl group. Figure 11 shows the TOFMS obtained when the methoxy group, rather than the methyl group, is deu-

TOFMS of 1-(methoxy- $d_3$ )-2-methylbenzene

**Figure 11.** TOFMS of the  $0_0^0$  region of 1-(methoxy- $d_3$ )-2-methylbenzene. The origin occurs at  $36\ 367.5\ \text{cm}^{-1}$ . The spacings between peaks are the same as in Figure 9. This observation rules out the assignment of any of the observed feature as transitions between torsional states of the methoxy group.

**Table VII.** Internal Rotational Levels for 1-Methoxy-2-methylbenzene in the  $S_1$  State<sup>a</sup>

level	energy ( $\text{cm}^{-1}$ )	level	energy ( $\text{cm}^{-1}$ )
$0a_1$	0.00	$3a_1$	55.12
$1e$	2.29	$4e$	83.42
$2e$	29.69	$5e$	125.74
$3a_2$	46.14		

<sup>a</sup>  $B = 4.76\ \text{cm}^{-1}$ ,  $V_3 = 49.07\ \text{cm}^{-1}$ ,  $V_6 = -6.20\ \text{cm}^{-1}$ .

**Table VIII.** Energies of Allowed Transitions between Internal Rotational Levels in the  $S_1$  States of 1-Methoxy-2-methylbenzene<sup>a</sup>

transition ( $S_0 \rightarrow S_1$ )	calcd $E$ ( $\text{cm}^{-1}$ )	obsd $E$ ( $\text{cm}^{-1}$ ) by TOFMS
$0a_1 \rightarrow 0a_1$	0.00	0
$0a_1 \rightarrow 3a_2$	46.14	47.5
$0a_1 \rightarrow 3a_1$	55.12	55.3
$1e \rightarrow 1e$	2.29	$\sim 2$
$1e \rightarrow 2e$	29.69	28.9
$1e \rightarrow 4e$	83.42	81.1
$1e \rightarrow 5e$	125.74	128.3

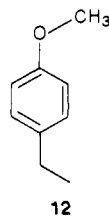
<sup>a</sup> The  $0a_1$  and  $1e$  levels in  $S_0$  are treated as being degenerate for the purposes of this calculation.

teriated. The 1-methyl-2-methoxybenzene and 1-(methoxy- $d_3$ )-2-methylbenzene (**11**) (Figure 11) have the same spacings between peaks. This result supports the assignment just outlined, and strongly implies that features due to transitions between torsional states of the methoxy group are not observed in the spectrum. We thus conclude that only a single  $0_0^0$  origin is observed for 1-methoxy-2-methylbenzene (**9**) and one each for **10** and **11**.

The DE spectra obtained by exciting the peaks in Figure 9 labeled a–e are presented in Figure 12a–e, respectively. The primary conclusion which can be drawn from these spectra is that the ring methyl group has a high ( $>300\ \text{cm}^{-1}$ ) barrier to rotation in the ground state  $S_0$ , because no methyl rotor torsional transitions are observed within  $100\ \text{cm}^{-1}$  of the origins in the DE spectra.

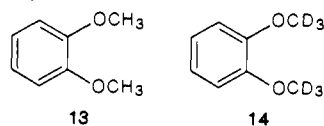
In contrast, the peaks in Figure 9 corresponding to excited-state ( $S_1$ ) levels can be fit to a fairly small barrier, with  $B = 4.76\ \text{cm}^{-1}$ ,  $V_3 = 49.07\ \text{cm}^{-1}$ , and  $V_6 = -6.2\ \text{cm}^{-1}$ . The energy levels are listed in Table VII, and the calculated and observed transition energies are listed in Table VIII.

**E. 1-Ethyl-4-methoxybenzene (12).** The TOFMS of the  $0_0^0$  region for  $S_1 \leftarrow S_0$  of jet-cooled 1-ethyl-4-methoxybenzene (**12**) is presented in Figure 13. The spectrum exhibits a single origin feature at  $35\ 572.9\ \text{cm}^{-1}$ . The feature at  $35\ 596.8\ \text{cm}^{-1}$  is due to torsional motion of the ethyl group and is similar to features observed in the spectra of other ethyl-substituted benzenes<sup>24</sup> (see below).



**F. Franck-Condon Factors for Methoxytoluenes.** The intensities of the various torsional features in Figures 3 and 5 should provide information about the relative angular displacement of the methyl group in the ground and excited electronic states. A calculation, similar to that done by Ito et al.<sup>33</sup> on *o*- and *m*-fluorotoluene, can be carried out using Franck-Condon overlap integrals evaluated from the eigenvectors associated with the various torsional energy levels. The phase shift between the potential functions and the wave functions in the ground and excited state is varied until the calculated relative intensities match those observed. While we are able to reproduce the results of Ito et al.<sup>33</sup> for the fluorotoluenes using their published data, we are not able to account for the intensity distributions in the spectra of the methoxytoluenes using only a simple overlap integral approach. For example, the methyl group of 1-methoxy-4-methylbenzene is almost freely rotating judging from the spacings of the torsional features in Figure 3 and from the symmetries indicated by the DE experiments. A low ( $\sim 10$  cm<sup>-1</sup>) barrier to methyl rotation in S<sub>1</sub> and S<sub>0</sub> is also expected from previous work on other para-substituted toluenes. If the barriers in S<sub>0</sub> and S<sub>1</sub> are indeed low, then the 0a<sub>1</sub> → 3a<sub>1</sub> transition intensity at  $\sim 54$  cm<sup>-1</sup> will be relatively unaffected by changes in phase between S<sub>1</sub> and S<sub>0</sub> and should be relatively weak compared to the origin. The fact that this transition has nearly half the intensity of the origin (Figure 3), however, indicates that some other mechanism, such as vibronic coupling, is affecting the transition intensities for this molecule. Similar conclusions can be drawn for 1-methoxy-3-methylbenzene.

**G. 1,2-Dimethoxybenzene (13).** The TOFMS of the 0<sub>0</sub><sup>0</sup> region for S<sub>1</sub> ← S<sub>0</sub> of 1,2-dimethoxybenzene (13) is presented in Figure 14. The spectrum contains what is undoubtedly an origin at 35 738.1 cm<sup>-1</sup>, and a profusion of intense features within the next 200 cm<sup>-1</sup>, labeled b-g. Examination of these features with DE (Figure 15b-g) reveals that they are all vibronics built on the origin (peak "a"). These low-lying features are presumably due to torsional motion of the methoxy group. To test this hypothesis the TOFMS of the methoxy-deuteriated analogue of 13, namely, 1,2-di(methoxy-d<sub>6</sub>)benzene (14), is obtained. This spectrum is



presented in Figure 16 and shows the same pattern of peaks as seen in Figure 14, except that the spacings have all shifted closer to the origin by an average of 8%.

Upon deuteration of the terminal methyl group of the methoxy substituent, the methyl rotational constant should be halved ( $\sim 5.2$  cm<sup>-1</sup> for OCH<sub>3</sub> to  $\sim 2.6$  cm<sup>-1</sup> for OCD<sub>3</sub>). The rotational constant for the entire methoxy group, however, should only change from  $\sim 1.0$  to 0.78 cm<sup>-1</sup> upon methoxy group deuteration. The latter difference is more consistent with the small change in shift observed in Figure 16 when the methoxy group is deuteriated. Thus features b-g in Figure 14 are assigned as being due to transitions between internal rotational states of the entire methoxy group. We thus conclude that only a single 0<sub>0</sub><sup>0</sup> origin transition is observed for 13.

Assignments for features b-g in Figure 14 are obtained based on the "double rotor" model previously employed for the xylenes.<sup>25</sup> A basis set consisting of 625 free rotor wave functions of the form,

$$\psi = e^{\pm im\phi} e^{\pm in\tau}$$

DE of 1-methoxy-2-methylbenzene

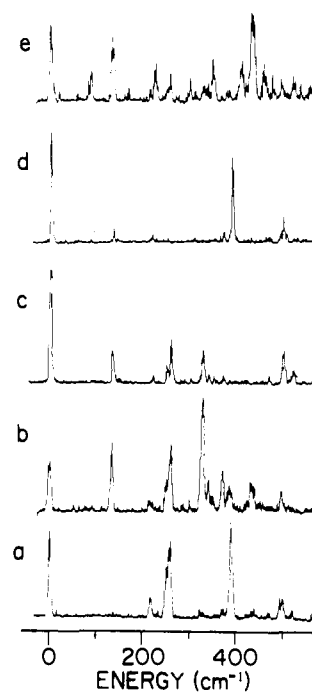


Figure 12. DE spectra of the 0<sub>0</sub><sup>0</sup> region of S<sub>0</sub> ← S<sub>1</sub> for 1-methoxy-2-methylbenzene, obtained by pumping the transitions labeled a-e in Figure 9. The absence of features within the first 100 cm<sup>-1</sup> of the origins indicates that the ring methyl rotor experiences a large (>200 cm<sup>-1</sup>) barrier to rotation in S<sub>0</sub>.

TOFMS of 1-ethyl-4-methoxybenzene

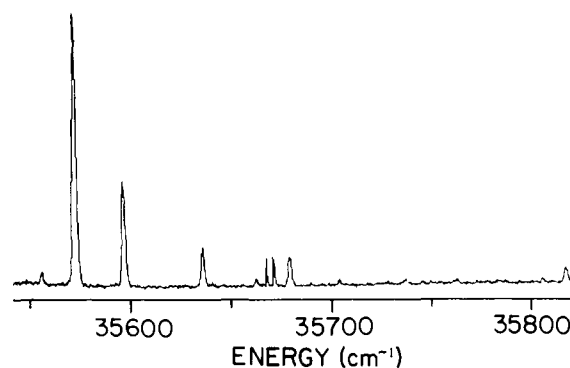
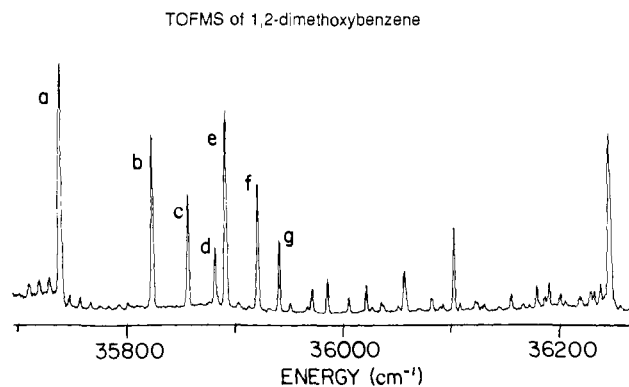


Figure 13. TOFMS of the 0<sub>0</sub><sup>0</sup> region of S<sub>1</sub> ← S<sub>0</sub> for 1-ethyl-4-methoxybenzene. The spectrum exhibits a single origin at 35 572.9 cm<sup>-1</sup>. This result helps to eliminate gauche conformations (3) of the methoxy group, relative to the ring, as energy minima.

in which  $n$  and  $m$  are the rotational quantum numbers, and  $\phi$  and  $\tau$  are the torsion angles (measured with respect to the plane of the ring). Both torsion angles ( $\tau$  and  $\phi$ ) are defined to maintain an identical "sense of rotation". If the lone pairs of electrons on the oxygen are ignored, then one of the methoxy groups will interact with the other once every 360° of rotation, and will interact with the benzene ring twice every 360° of rotation. These interactions can therefore be represented by  $V_1$  and  $V_2$  potential terms of the form,<sup>25</sup>

$$V(\phi, \tau) = \sum_n \frac{1}{2} [V_n (2 - \cos n\tau - \cos n\phi + V_n' (\cos(n\tau - n\phi)) - 2)]$$

If potential interactions involving the lone pairs of electrons need to be accounted for, then  $V_3$  and  $V_6$  potential terms, in addition to  $V_1$  and  $V_2$  terms, need to be added to the expansion. Cross potential ( $V_n'$ ) and kinetic ( $\chi$ ) terms may also be necessary to



**Figure 14.** TOFMS of the  $0_0^0$  region of  $S_1 \leftarrow S_0$  for 1,2-dimethoxybenzene. The single origin of the spectrum, at  $35738.1 \text{ cm}^{-1}$ , is labeled "a". Peaks b-g are vibronic bands, presumably due to torsional motion of the methoxy group.

**Table IX.** Internal Rotational Levels of the Methoxy Groups of 1,2-Dimethoxybenzene in  $S_1$

level	energy ( $\text{cm}^{-1}$ ) <sup>a</sup>	obsd energy ( $\text{cm}^{-1}$ )	level	energy ( $\text{cm}^{-1}$ ) <sup>a</sup>	obsd energy ( $\text{cm}^{-1}$ )
$0a_1$	0.00	0	$11a_2$	164.28	
$1a_2$	38.29		$12a_1$	165.56	152.3
$2a_2$	60.09		$13a_2$	167.50	
$3a_1$	75.98	84.4	$14a_2$	169.04	
$4a_2$	93.10		$15a_2$	184.14	
$5a_2$	112.03		$16a_1$	188.42	181.7
$6a_1$	115.15	117.6	$17a_2$	189.25	
$7a_2$	123.20		$18a_2$	191.04	
$8a_2$	141.49		$19a_2$	203.71	
$9a_1$	143.52	142.8	$20a_1$	208.08	201.4
$10a_2$	148.15				

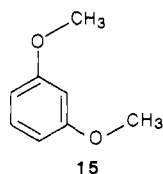
<sup>a</sup>  $B = 1.0 \text{ cm}^{-1}$ ,  $V_1 = 500 \text{ cm}^{-1}$ ,  $V_2 = -50 \text{ cm}^{-1}$ ,  $V_3 = 100 \text{ cm}^{-1}$ ,  $V_6 = 50 \text{ cm}^{-1}$ ,  $V_1' = -150 \text{ cm}^{-1}$ ,  $\chi = 0.9$ .

describe the potential for the dimethoxy substitution.

The molecular symmetry group<sup>32,34</sup> of 1,2-dimethoxybenzene is  $G_4$  if rotation of the methyl of the methoxy group is ignored. The symmetries of the torsional levels of the entire methoxy group are  $A_1$  and  $A_2$ .  $A_1 \leftrightarrow A_2$  transitions are symmetry forbidden, and only  $A_1 \leftrightarrow A_1$  transitions should appear in the spectrum.

Table IX lists the energy levels obtained for  $V_1 = 500 \text{ cm}^{-1}$ ,  $V_2 = -50 \text{ cm}^{-1}$ ,  $V_3 = 100 \text{ cm}^{-1}$ ,  $V_6 = 50 \text{ cm}^{-1}$ ,  $V_1' = -150 \text{ cm}^{-1}$ ,  $\chi = 0.9$ , and  $B = 1.0 \text{ cm}^{-1}$  which match the observed spacings observed in Figure 14 reasonably well. The calculated zero-point energy is  $164.0 \text{ cm}^{-1}$ .

**H. 1,3-Dimethoxybenzene (15) and 1,4-Dimethoxybenzene (16).** The TOFMS of the  $0_0^0$  region for  $S_1 \leftarrow S_0$  of 1,3-dimethoxybenzene (15) is presented in Figure 17. The DE spectra of the



peaks labeled a-g in this spectrum are presented in Figure 18a-g, respectively. These spectra reveal that the features labeled d through g in Figure 17 are vibronics built on the origin at  $36101.5 \text{ cm}^{-1}$  (labeled a). The DE spectra for peaks b and c are unique; we conclude that peaks b and c are separate origins along with peak a.

Peaks d-g in Figure 17 can also be expected to be due to torsional transitions of the entire methoxy group. If this is the case, then the fact that the first such transition takes place  $\sim 190 \text{ cm}^{-1}$  from the origin indicates that the potential barrier to methoxy

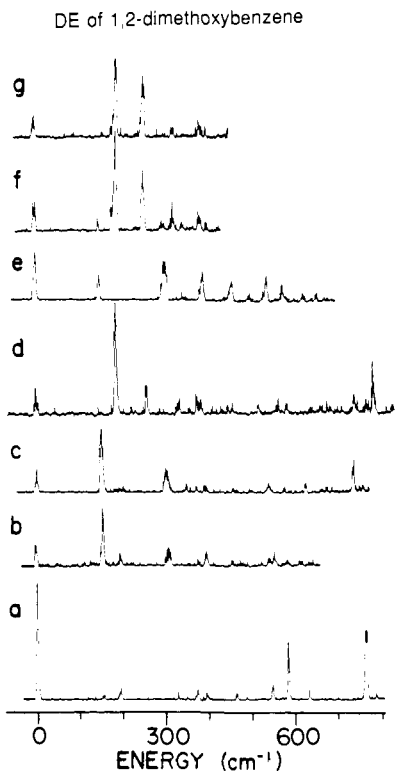


**Figure 15.** DE spectra of the  $0_0^0$  region of  $S_0 \leftarrow S_1$  for 1,2-dimethoxybenzene, obtained by pumping features a-g in Figure 14. The intensity distributions in spectra b-g indicate that the pumped transitions b-g in Figure 14 are all vibronics built on the origin.

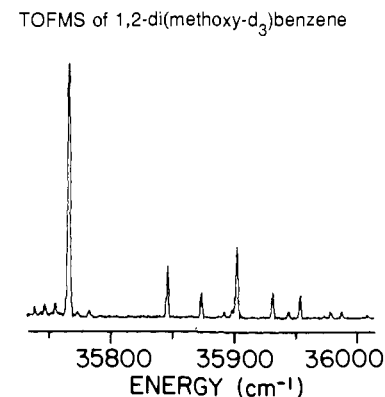
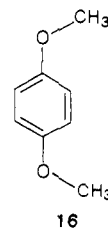


**Figure 16.** TOFMS of the  $0_0^0$  region of  $S_1 \leftarrow S_0$  for 1,2-(dimethoxy- $d_3$ )benzene. The origin occurs at  $35767.1 \text{ cm}^{-1}$ . The spectrum is quite similar to the first part of Figure 14, except that the spacings between peaks are smaller, consistent with the smaller rotational constant of the deuteriated methoxy group.

rotation in this molecule must be on the order of  $2000\text{--}5000 \text{ cm}^{-1}$ . This is a substantially higher barrier than in 1,2-dimethoxybenzene. 1,4-Dimethoxybenzene (16) has been studied previously<sup>8,9</sup> and two  $0_0^0$  transitions were observed.



#### IV. Discussion

**A. The Methoxy Group Conformation.** The minimum energy conformation of a methoxy group substituted on a benzene ring is clearly established by the number of origins observed for the

(34) Longuet-Higgins, H. C. *Mol. Phys.* **1963**, *6*, 445.



**Table X.** Number of Conformations of Various Aryl Methyl Ethers Based on Experiment and Conformational Analysis Predictions

compound	number of conformations			experimentally observed
	predicted <sup>a</sup>			
	1 planar	2 perpendicular	3 gauche	
anisole (4)	1	1	1	1
1-methoxy-2-methylbenzene (9)	2 <sup>b</sup>	1 <sup>b</sup>	2 <sup>b</sup>	1
1-methoxy-3-methylbenzene (6)	2	1	2	2
1-methoxy-4-methylbenzene (5)	1	1	1	1
1-ethyl-4-methoxybenzene (12)	1	2	2	1
1,2-dimethoxybenzene (13)	3 <sup>b</sup>	2 <sup>b</sup>	7 <sup>b</sup>	1
1,3-dimethoxybenzene (15)	3	2	7	3
1,4-dimethoxybenzene (16)	2	2	4	2 <sup>c</sup>

<sup>a</sup> Based on counting all possible molecular conformations having the particular substituent conformation, but counting degenerate conformations only once. <sup>b</sup> For 1,2-disubstituted substrates, steric effects would certainly render some conformations energetically unfavorable. Hence, this prediction must be considered the maximum number possible. See text and ref 3 for further discussion. <sup>c</sup> From ref 8 and 9.

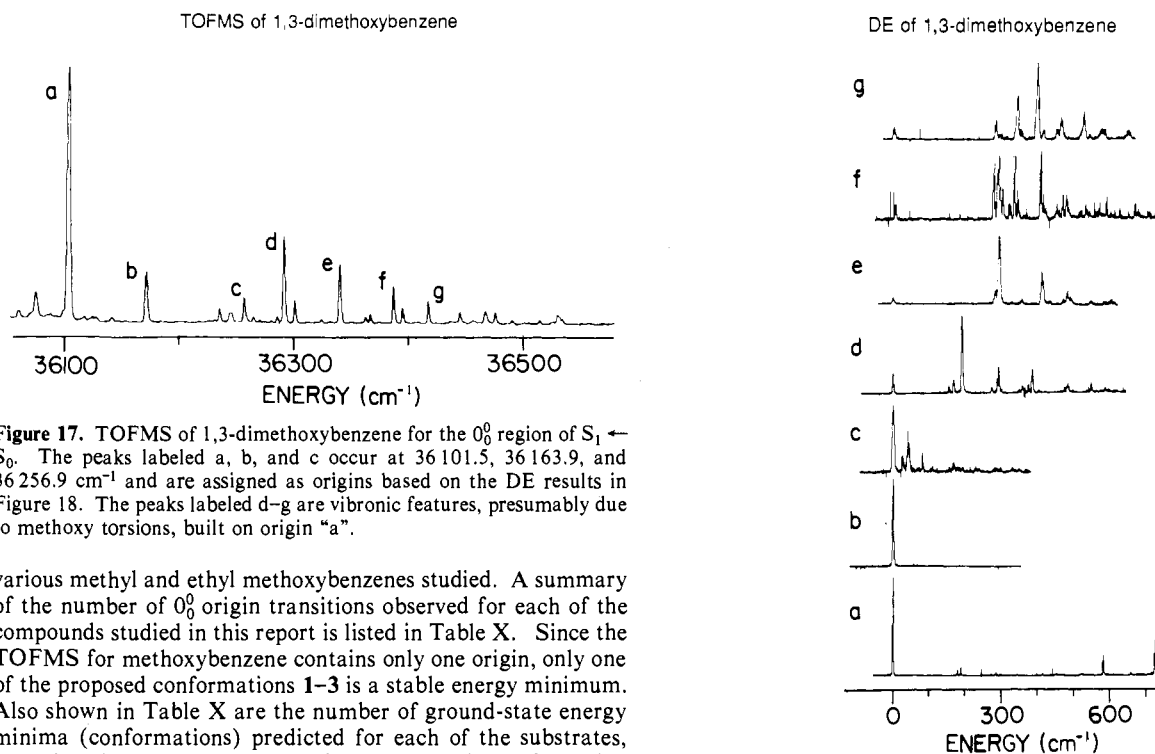
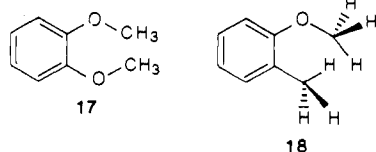


**Figure 17.** TOFMS of 1,3-dimethoxybenzene for the  $0_0^0$  region of  $S_1 \leftarrow S_0$ . The peaks labeled a, b, and c occur at 36 101.5, 36 163.9, and 36 256.9  $\text{cm}^{-1}$  and are assigned as origins based on the DE results in Figure 18. The peaks labeled d–g are vibronic features, presumably due to methoxy torsions, built on origin “a”.

various methyl and ethyl methoxybenzenes studied. A summary of the number of  $0_0^0$  origin transitions observed for each of the compounds studied in this report is listed in Table X. Since the TOFMS for methoxybenzene contains only one origin, only one of the proposed conformations 1–3 is a stable energy minimum. Also shown in Table X are the number of ground-state energy minima (conformations) predicted for each of the substrates, assuming either a planar, perpendicular, or gauche conformation for the methoxy substituent. The predicted values are based entirely on “counting” the various possible combinations of conformations for the individual substituents, excluding rotational characteristics of the methyl hydrogens themselves.

Examination of Table X indicates that no set of predictions based on one of 1–3 conformations matches the observed number of conformations in all cases. This is as expected, since steric effects in all 1,2-disubstituted benzenes would render some of the predicted conformations to be significantly destabilized and thus depopulated.<sup>13,15</sup> Hence, the predictions for 1-methoxy-2-methylbenzene (9) and 1,2-dimethoxybenzene (13) must be modified (i.e., decreased) to remove from consideration unstable conformations such as illustrated by 17 and 18.

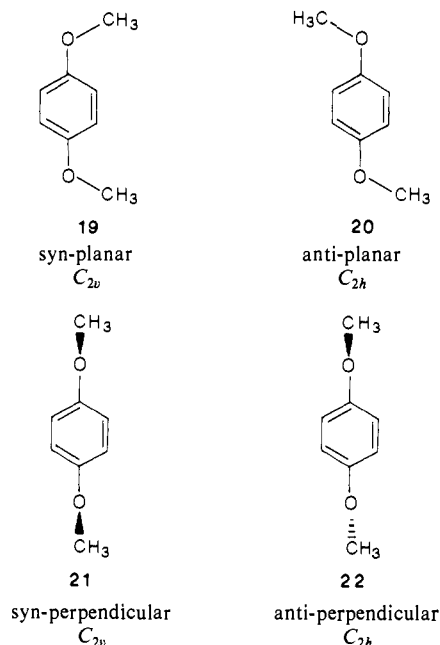


To distinguish among 1–3, the data for 9 and 13 should be excluded as we would have to know unequivocally relative energies

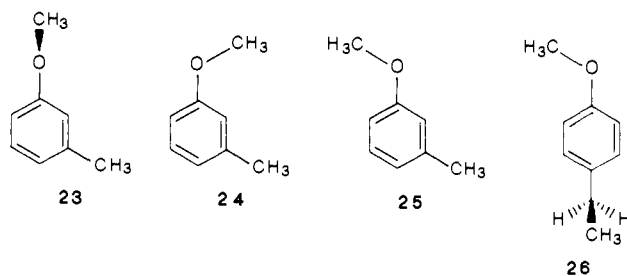
**Figure 18.** DE spectra of the  $0_0^0$  region of  $S_0 \leftarrow S_1$  for 1,3-dimethoxybenzene obtained by pumping the transitions labeled a–g in Figure 17. The uniqueness of spectra a–c in this figure lead to the assignment of peaks a–c in Figure 17 as separate origins. The lack of intensity at the origins of spectra d–g, plus their similarities with each other and with “a” lead to the assignments of features d–g in Figure 17 as methoxy torsions built on the origin “a”.

of their different conformations. The data for the other six substrates (4–6, 12, 15, and 16) are consistent only with the planar conformation 1 for the aryl methyl ether moiety.

The detailed logic involved in this structural conclusion is now presented. Consider first the case of 1,4-dimethoxybenzene (16). Two origin transitions were first observed by Oikawa, et al.<sup>8</sup>, and based on symmetry arguments, they assigned the ground-state conformation of 16 to be the all-planar conformations syn-planar 19 and anti-planar 20. Alternatively, the syn-perpendicular 21 and the anti-perpendicular 22 could obtain. As 19 and 21 have identical symmetries (both  $C_{2v}$ ), and as 20 and 22 have identical symmetries (both  $C_{2h}$ ), a unique conformational assignment cannot be made using the data of Oikawa et al.<sup>8</sup> In other words, the TOFMS of 16 serves only to exclude gauche conformations related to 3 but cannot distinguish between the planar 1 and perpendicular 2 conformations.



Consider the TOFMS of 1-methoxy-3-methylbenzene and 1-ethyl-4-methoxybenzene. The TOFMS of 1-methoxy-3-methylbenzene contains two origins; this observation eliminates the perpendicular conformation **23** as a possible structure, since this conformer can give rise to only one unique geometry and therefore only one origin. These two origins obtain from conformers **24** and **25**. For 1-ethyl-4-methoxybenzene (**12**), a gauche



conformation of the methoxy group would yield two distinct conformations and two origins in the TOFMS, given that the ethyl group projects up out of the plane of the ring in a perpendicular conformation.<sup>24</sup> A planar conformation of the methoxy group in this compound yields only one unique geometry, and therefore only one origin would be expected in the TOFMS. As stated earlier, this is, in fact, what is observed; the TOFMS of 1-ethyl-4-methoxybenzene contains a single origin. Hence, conformation **26** must be the minimum energy conformation for **12**, and a planar conformation is present for an unhindered methoxy group substituted on an aromatic ring.

As discussed above, we cannot unambiguously define the conformations of 1-methoxy-2-methylbenzene (**9**) and 1,2-dimethoxybenzene (**13**). In each of these two cases, only a single origin is observed. Assuming that no kinetic effect<sup>24,25,35</sup> is operative which depopulates additional ground-state energy minima, both **9** and **13** exist in a single conformation in the gas phase. Some controversy exists with regard to **13**. Kollman, Houk, et al.<sup>11</sup> concluded that **13** exists in nonplanar conformations in the gas phase, based on photoelectron spectroscopic studies and ab initio STO-3G calculations. Subsequently, Makriyannis and Fesik<sup>10</sup> and independently Schaefer and Laatikainen<sup>19</sup> concluded that **13** exists in the planar conformation in solution phase based on rather elegant and sophisticated NMR studies.<sup>36</sup>

One is tempted to use the relative intensities of the origin transitions of the various methoxy-substituted benzenes and toluenes to suggest relative populations of the different conformers; however, a comparison of Figures 5, 7, and 8 will show that, in this system, relative origin intensities are governed by complicated couplings, interactions, and overlaps that preclude such simple generalizations.

**B. Methyl and Methoxy Internal Dynamics.** The potential parameters for methyl rotation in the methyl anisoles are quite different from those observed for the somewhat analogous hydrocarbons such as the ethyltoluenes.<sup>24</sup> The intensity distributions in the TOFMS of the methoxytoluenes are also quite unusual. The potential barrier for 1-methoxy-4-methylbenzene decreases on going from  $S_0$  to  $S_1$ , and the methyl rotor transitions are intense even though the methyl group is essentially a free rotor. The methoxy group must change the electron densities in the molecule when the molecule is excited to  $S_1$ , resulting in changes in the methyl rotational constant, vibronic coupling, etc. Also note that  $V_3$  for  $S_0$  is larger than  $V_6$ , but the reverse is true in  $S_1$ : we cannot thus readily attribute the relative  $V_3/V_6$  sizes to bulk steric effects associated with the methoxy group planar configuration in 1-methoxy-4-methylbenzene. 1-Methoxy-3-methylbenzene has a relatively large barrier to methyl rotation, while the para and ortho isomers have relatively low barriers. This fact must also be related to some type of hyperconjugative electronic effect, the details of which we do not currently understand.

The results obtained from the dimethoxybenzenes also suggest a much larger barrier to, in this case, rotation of the methoxy group in the meta isomer as compared to the ortho isomer; the same electronic effect mentioned for the methoxytoluenes must also be operative for the dimethoxy compounds. The large barriers to methoxy rotation, along with the presence of substantial cross kinetic and potential terms, indicate that the methoxy groups in 1,2- and 1,3-dimethoxybenzene interact strongly.

The geometry of the minimum energy conformation of the methoxy groups in 1,2- and 1,3-dimethoxybenzene may well change upon electronic excitation, since these are the only methoxy-substituted benzenes studied which exhibit methoxy torsional transitions in the TOFMS. (The TOFMS of 1,4-dimethoxybenzene was observed to exhibit only two origins and no low-lying torsional structure, in accordance with results reported by Ito et al.<sup>8,9</sup>) Methoxybenzene and the methoxytoluenes, as well as 1,4-dimethoxybenzene, do not exhibit methoxy torsional transitions in the TOFMS because the geometry of the methoxy group is unchanged upon excitation from  $S_0$  to  $S_1$ , and the resulting Franck-Condon overlaps are too small for the methoxy torsional transitions to appear with any intensity in the spectrum. Thus, steric hindrance between the methoxy groups in 1,2- and 1,3-dimethoxybenzene may be forcing the methoxy groups to change geometry (and orientation) upon electronic excitation.

## V. Conclusions

The results presented in this paper are important in terms of three specific contributions. First, by observing specific origin transitions for these aryl methyl ethers, we have experimentally observed spectroscopic properties of the frozen-out conformations. Second, by using structural and symmetry arguments, we have been able to demonstrate that the methoxy substituent on an aromatic ring lies in the plane of the ring, in the absence of overriding steric effects from substituents on adjacent ring positions. Third, by fitting the experimental spectral data to a rigid rotor model, we have been able to quantify the barriers to internal rotation for methyl and methoxy substituents in the various methoxytoluenes and dimethoxybenzenes in both the  $S_0$  and  $S_1$  electronic states. The barrier to rotation is particularly high for either group in the 1,3 or meta position due to a methoxy electronic induction effect. The unusual spectroscopic intensity patterns

(35) Seeman, J. I.; Secor, H. V.; Breen, P. J.; Grassian, V. H.; Bernstein, E. R. *J. Am. Chem. Soc.*, in press.

(36) Note Added In Proof: For a recent study of "conformational flexibility of the methoxyphenyl group studied by statistical analysis of crystal structure data", including an excellent discussion of the observation of perpendicular (2) conformations in sterically hindered cases, see ref 3a.

observed in these systems suggest that the  $S_0$  and  $S_1$  states of methoxy-substituted benzenes and toluenes may be quite different, much more so than has been observed for alkyl-substituted benzenes.

**Acknowledgment.** We thank J. Campbell for obtaining the NMR spectra, J. Paine for helpful discussions, and R. Ferguson, A. Kassman, A.C. Lilly, and B. LaRoy for their support and encouragement. This work was supported in part by ONR.

Registry No. 4, 100-66-3; 5, 104-93-8; 6, 100-84-5; 9, 578-58-5; 12, 1515-95-3; 13, 91-16-7; 15, 151-10-0; 16, 150-78-7.

**Supplementary Material Available:** Experimental procedures for the preparation of 1-methoxy-3-(methyl- $d_3$ )benzene<sup>29</sup> (7), 1-(methoxy- $d_3$ )-3-methylbenzene<sup>30</sup> (8), 1-methoxy-2-(methyl- $d_3$ )benzene (10), 1-(methoxy- $d_3$ )-2-methylbenzene (11), and 1,2-di(methoxy- $d_3$ )benzene<sup>31</sup> (14) (3 pages). Ordering information is given on any current masthead page.

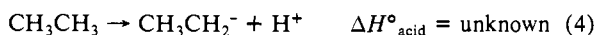
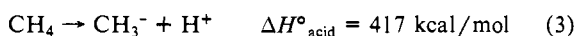
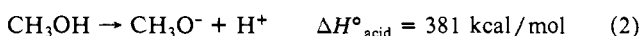
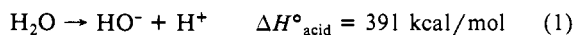
## The Gas-Phase Acidities of the Alkanes

Charles H. DePuy,<sup>\*,†</sup> Scott Gronert,<sup>†</sup> Stephan E. Barlow,<sup>†</sup> Veronica M. Bierbaum,<sup>†</sup> and Robert Damrauer<sup>\*,†</sup>

Contribution from the Department of Chemistry and Biochemistry, University of Colorado, Boulder, Colorado 80309-0215, and the Department of Chemistry, University of Colorado at Denver, Denver, Colorado 80204. Received July 5, 1988

**Abstract:** The gas-phase acidities of 15 simple alkanes have been determined in a flowing afterglow-selected ion flow tube (FA-SIFT) by a kinetic method in which alkyltrimethylsilanes are allowed to react with hydroxide ions to produce a mixture of trimethylsiloxide ions by loss of alkane and alkyltrimethylsiloxide ions by loss of methane. The reaction is proposed to proceed by addition of hydroxide ion to the silane to form a pentacoordinate silicate ion intermediate which decomposes through two transition states, one in which negative charge is placed on a methyl group and the other in which negative charge is placed on the alkyl group. The ratio of siloxide ions produced is proposed to be correlated to the relative basicity of the methyl and alkyl anions. The method is calibrated by making use of the known acidities of methane ( $\Delta H^\circ_{\text{acid}} = 416.6$  kcal/mol) and benzene ( $\Delta H^\circ_{\text{acid}} = 400.7$  kcal/mol). In general, methyl substitution is found to stabilize alkyl anions in the gas phase except that the ethyl anion is found to be more basic than the methyl anion. By combining the gas-phase acidities with the bond dissociation energies, the electron affinities (EA) of the corresponding alkyl radicals can be calculated. Many simple alkyl radicals are found to have negative EA's. The results for the alkyl groups studied are as follows, where the first number is the  $\Delta H^\circ_{\text{acid}}$  (kcal/mol) of the corresponding alkane and the second number (in parentheses) is the EA (kcal/mol) of the alkyl radical: ethyl 420.1 (-6.4), isopropyl 419.4 (-9.5), cyclobutyl 417.4 (-7.5), cyclopentyl 416.1 (-7.0), *sec*-butyl 415.7 (-5.8), *n*-propyl 415.6 (-1.9), *tert*-butyl 413.1 (-5.9), isobutyl 412.9 (0.8), 3-butenyl 412.0 (1.7), cyclopropyl 411.5 (8.4), cyclopropylmethyl 410.5 (3.2), 1-methylcyclopropyl 409.2 (8.0), neopentyl 408.9 (4.8), vinyl 407.5 (16.1), and 2-propenyl 405.8 (15.8).

With the single exception of methane, the gas-phase acidities of the alkanes have not been determined,<sup>1</sup> and little more is known about their acidities in solution.<sup>2</sup> The problem is an experimental one; with few exceptions<sup>3-5</sup> alkyl anions have not been detected in the gas phase so that it has not been possible to apply the usual methods for determining their basicity. Yet such a determination would be of great fundamental interest, for it could, in principle, reveal a great deal about the electronic structures of simple anions. The problem is especially intriguing because theoretical calculations are, to some extent, at variance with experimental analogies. For example, replacement of a hydrogen atom in water by a methyl group to produce methanol results in a 10-kcal/mol increase in acidity.<sup>6</sup> Yet a number of high-level ab initio calculations<sup>7</sup> and a few investigations on carbanion salts in solution<sup>2</sup> indicate that the analogous substitution in the alkane series, from methane to ethane, will result in an acidity decrease.



In view of the failure of the standard methods for determining the acidity of these extremely weak acids, we were led to search for an alternative method which might prove useful as a general

tool for investigating substituent effects on the acidity of alkanes. We reported preliminary results of our investigations in an earlier paper.<sup>8</sup> In the meantime we have made substantial instrumental improvements which greatly increase the accuracy of our results. In addition, we have extended our method to a much greater number of compounds so that a better analysis of substitution patterns can emerge.

Our method for determining the gas-phase acidities of the alkanes is a kinetic one based on a linear free energy relationship and grew out of our studies of the gas-phase anion chemistry of silanes.<sup>9</sup> We first used trimethylsilyl derivatives of organic

(1) Lias, S. G.; Bartmess, J. E.; Liebman, J. F.; Holmes, J. L.; Levin, R. D.; Mallard, W. G. *J. Phys. Chem. Ref. Data* 1988, 17, Suppl. 1.

(2) (a) Streitwieser, A., Jr.; Juaristi, E.; Nebenzahl, L. L. In *Comprehensive Carbanion Chemistry, Part A*; Bunce, E., Durst, T., Eds.; Elsevier: Amsterdam, 1980; Chapter 7. (b) Streitwieser, A., Jr.; Taylor, D. R. *J. Chem. Soc., Chem. Commun.* 1970, 1248. (c) Dessy, R. E.; Kitching, W.; Psarras, T.; Salinger, R.; Chen, A.; Chivers, T. *J. Am. Chem. Soc.* 1966, 88, 460. (d) Applequist, D. E.; O'Brien, P. F. *J. Am. Chem. Soc.* 1963, 85, 743.

(3) Ellison, G. B.; Engelking, P. C.; Lineberger, W. C. *J. Am. Chem. Soc.* 1978, 100, 2556.

(4) Graul, S. T.; Squires, R. R. *J. Am. Chem. Soc.* 1988, 110, 607.

(5) Froelicher, S. W.; Freiser, B. S.; Squires, R. R. *J. Am. Chem. Soc.* 1986, 108, 2853.

(6) Brauman, J. I.; Blair, L. K. *J. Am. Chem. Soc.* 1970, 92, 5986.

(7) (a) Kollmar, H. *J. Am. Chem. Soc.* 1978, 100, 2665. (b) Schleyer, P. v. R.; Spitznagel, G. W.; Chandrasekhar, J. *Tetrahedron Lett.* 1986, 27, 4411. (c) Siggel, M. R.; Thomas, T. D.; Saethre, L. J. *J. Am. Chem. Soc.* 1988, 110, 91. (d) Jorgensen, W. L.; Briggs, J. M.; Gao, J. *J. Am. Chem. Soc.* 1987, 109, 6857.

(8) DePuy, C. H.; Bierbaum, V. M.; Damrauer, R. *J. Am. Chem. Soc.* 1984, 106, 4051.

(9) DePuy, C. H.; Damrauer, R.; Bowie, J. H.; Sheldon, J. C. *Acc. Chem. Res.* 1987, 20, 127.

<sup>†</sup> University of Colorado—Boulder.

<sup>†</sup> University of Colorado—Denver.